CRYSTAL GROWTH & DESIGN

pubs.acs.org/crystal

Article

Synthesis of Coordination Polymers and Discrete Complexes from the Reaction of Copper(II) Carboxylates with Pyrazole: Role of Carboxylates Basicity

Rebecca Scatena,* Sara Massignani, Arianna E. Lanza, Federico Zorzi, Magda Monari,* Fabrizio Nestola, Claudio Pettinari, and Luciano Pandolfo*

Cite This: *Cryst. Growth Des.* 2022, 22, 1032−1044

Read Online

ACCESS | Metrics & More | Article Recommendations | Supporting Information

ABSTRACT: The reaction of select copper(II) monocarboxylates $Cu(RCOO)_2(H_2O)_x$ (R = C_4H_3O, C_6H_5, H; x = 2, 4) with pyrazole (Hpz), carried out in protic solvents, yields mono- or dinuclear species $[Cu(RCOO)_2(Hpz)_n]_m$ (n = 2, 4; m = 1, 2), always accompanied by tri- or hexanuclear derivatives based on the triangular $[Cu_3(\mu_3\text{-}OH)(\mu\text{-}pz)_3]^{2+}$ fragment. The molecular structures of all isolated compounds have been established through XRD determinations. In some cases, the mono-, or dinuclear species act as secondary building units, self-assembling into 1D or 3D coordination polymers. The hexanuclear benzoate cluster contains coordinated and crystallization MeOH molecules, whose removal generates a crystalline 1D coordination polymer that can be reconverted into the hexanuclear cluster by soaking in MeOH. The relatively high pK_b values of carboxylate anions employed in the syntheses are responsible for the preferential formation of mono- or dinuclear species rather than tri- or hexanuclear ones.

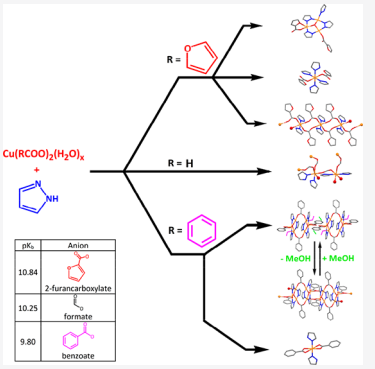

INTRODUCTION

Design and optimization of functional coordination polymers (CPs) is based on structure−property relationships that permit to foresee the contribution of building blocks, functional groups, guest molecules, and their interaction to the overall properties.[1−5] However, the following realization of desired structural topologies incorporating selected components is not just governed by choice of geometry, size, conformation, and number and nature of the binding sites of the building blocks,[6,7] but it also critically depends on reaction conditions that control their self-assembly.[8−13] Therefore, progress in the development of targeted materials requires the rationalization and generalization of the effect of fundamental parameters that may be used to *a priori* design and drive the synthesis.

Taking into account that azolates are polytopic synthons suitable to generate CPs frameworks[14−22] and that monocarboxylate ions may bridge up to four metal ions, in recent years, we have studied the effect of reaction conditions on the interaction of copper(II) carboxylates with N-donor ligands. In detail, the reaction of some Cu^{II} monocarboxylates with pyrazole (Hpz) in dry MeCN leads to the 1D CP $[Cu(pz)_2]$,[23−25] a flexible framework showing a "porosity without pore" behavior.[26] On the contrary, by performing the same reaction in protic solvents and in the presence of water, 1D and 2D CPs, where monocarboxylate ions bridge two trinuclear triangular moieties $[Cu_3(\mu_3\text{-}OH)(\mu\text{-}pz)_3]^{2+}$ (Chart 1), formed.[27−32] A possible reaction mechanism for the formation of the trinuclear triangular species was proposed in ref 33.

Chart 1. $[Cu_3(\mu_3\text{-}OH)(\mu\text{-}pz)_3]^{2+}$ Trinuclear Triangular Moiety

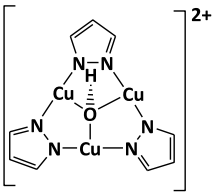

Recently, we have reported that the basicity of carboxylates appears to play a primary role in controlling the formation of trinuclear triangular species in protic solvents. Carboxylate anions having pK_b values in the range 8.97−9.69 drive the reaction of corresponding copper salts with Hpz toward the almost exclusive synthesis of trinuclear systems.[34] This result can be understood in terms of their ability to efficiently

Received: July 30, 2021
Revised: December 15, 2021
Published: December 30, 2021

https://doi.org/10.1021/acs.cgd.1c00861
Cryst. Growth Des. 2022, 22, 1032−1044

deprotonate water and Hpz forming OH^- and pz^- anions needed in the self-assembly of the $[Cu_3(\mu_3\text{-}OH)(\mu\text{-}pz)_3]^{2+}$ moiety. On the contrary, the reactions of weakly basic copper(II) salts with Hpz generate only mononuclear pyrazole complexes, in analogy to the behavior observed with copper(II) trifluoroacetate (pK_b = 13.48).[27] Possibly, the relatively high pK_b value (10.25) of the formate ion could also be the reason for the relatively low yield (*ca.* 20%) in the synthesis of the trinuclear species $[Cu_3(\mu_3\text{-}OH)(\mu\text{-}pz)_3(HCOO)_2(Hpz)_2]\cdot H_2O$, **A**,[28] with respect to the yields of other analogous derivatives with different carboxylates.[27−32,34] Moreover, we reported that by reacting copper(II) chloroacetate [$Cu(Clac)_2$, pK_b = 11.13] with Hpz, a 1D CP based on the mononuclear $Cu(\mu\text{-}Clac)_2(Hpz)_2$ node is mainly produced, accompanied by small quantities of a trinuclear and a dinuclear derivative, the latter being obtained through a peculiar dehydrochlorination reaction.[35]

It is noteworthy that $[Cu_3(\mu_3\text{-}OH)(\mu\text{-}pz)_3]^{2+}$ fragments have been employed as unusual synthons to generate polydimensional CPs, by connecting them through neutral N-donor ligands[36−41] or bicarboxylate anions.[38,42−47] Recently, derivatives containing the trinuclear triangular Cu^{II} pyrazolate fragment have been reported as low-melting salts having controllable magnetic properties[48] or interesting magneto structural aspects[49] or have been employed as secondary building units (SBUs) to obtain multifunctional MOFs[50] or 2D bimetallic MOFs.[51]

Continuing our studies, we report here on the results of the reactions of three select copper(II) carboxylates [2-furancarboxylate (Furc), formate (Form), and benzoate (Bnz), Chart 2], with Hpz in protic solvents. These syntheses were designed

Chart 2. Carboxylate Anions Employed in the Syntheses with Their pK_b Values Indicated in Parentheses[52]

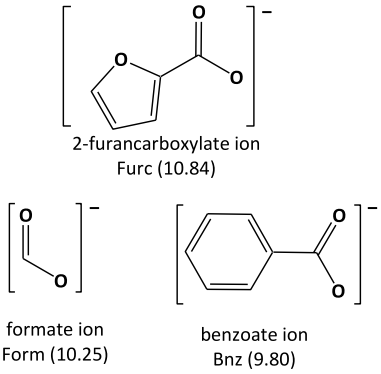

to finally determine the influence of carboxylates basicity on the reaction route and obtain new mono- or polynuclear Cu^{II} species, possibly assembled to form CPs.

EXPERIMENTAL SECTION

Materials and Methods. All the reactions and manipulations were carried out in air. Copper(II) formate was purchased from Aldrich and used without further purification. Copper(II) benzoate, $[Cu(Bnz)_2(H_2O)_2]\cdot H_2O$, was prepared according to ref 53. Elemental analyses (C, H, N) were performed with a Fisons Instruments 1108 CHNS-O elemental analyzer. Infrared spectra from 4000 to 600 cm^{-1} were recorded with a PerkinElmer Spectrum One Model FTIR spectrometer with ATR mode. The magnetic susceptibilities were measured at room temperature (20−28 °C) with a Sherwood Scientific magnetic balance MSB-Auto, using $HgCo(NCS)_4$ as calibrant and corrected for diamagnetism with the appropriate Pascal constants. The magnetic moments (in μB) were calculated from the equation $\mu_{eff} = 2.84(X_m^{corr}T)^{1/2}$.

Crystallographic Data Collection and Structure Determination. Single crystal X-ray diffraction (SCXRD) experiments were performed at room temperature (except for **3h**, which was measured at 173 K), with area detector diffractometers and Mo Kα radiation. The integrated intensity data were corrected for Lorentz, polarization, and absorption effects, and they were employed for structure solution and refinement. When the sample was not suitable for SCXRD measurements, powder X-ray diffraction (PXRD) was executed on a Panalytical X'Pert Pro diffractometer equipped with Cu Kα radiation. The experimental procedures (a, b, or c), and data treatment (d or p) are described in detail in the Supporting Information.

Molecular graphics were generated by using the program Mercury 2020.2.0.[54,55] Color codes for all molecular graphics: yellow-orange (Cu), blue (N), red (O), gray (C), and white (H). Crystal data and details of data collections for compounds **1**−**3** are reported in Table 1. Throughout the text, in the labeling of isolated compounds we have adopted, besides the **1**−**3** digits (2-furancarboxylates, formates and benzoates derivatives, respectively), the letters **m**, **d**, **t**, and **h** to indicate the mono-, di, tri-, and hexanuclear metal assemblies. Moreover, we have employed the $_4$ and $_2$ subscripts to distinguish between the two different mononuclear 2-furancarboxylates derivatives coordinating, respectively, four and two Hpz molecules.

SYNTHESES

Synthesis of $[Cu(Furc)_2(H_2O)_2]$. To a solution of 7.92 g of 2-furancarboxylic acid (70.6 mmol) in 120 mL of water, $Cu(CO_3)Cu(OH)_2$ (3.38 g, 15.25 mmol) was slowly added. The suspension was stirred overnight and then the solid was filtered, washed with water and dried under vacuum, obtaining 5.31 g of a blue-green powder. Yield: 54%. Anal. (%) Calcd for $Cu(Furc)_2(H_2O)_2$: C = 37.33; H = 3.13. Found: C = 37.23; H = 3.22. IR (ATR, cm^{-1}): 3430, 3156, 1606, 1584, 1478, 1417, 1372, 1230, 1200, 1146, 1081, 1012, 936, 883, 809, 780, 756. μ_{eff} (292 K) = 1.982 μ_B (calculated for $C_{10}H_{10}CuO_8$).

Reactions of Copper(II) Carboxylates with Hpz. *Reaction of $[Cu(Furc)_2(H_2O)_2]$ + Hpz in MeOH. Synthesis of $[Cu_3(\mu_3\text{-}OH)(\mu\text{-}pz)_3(Furc)_2(Hpz)]\cdot H_2O$,* ***1t****, $[Cu(Furc)_2(Hpz)_4]$,* ***1m$_4$****, and $[Cu(Furc)_2(Hpz)_2]$,* ***1m$_2$****.* To a solution of $[Cu(Furc)_2(H_2O)_2]$ (1.002 g, 3.12 mmol) in 100 mL of MeOH, a solution of 588 mg of Hpz (8.65 mmol) in 10 mL of MeOH was added under stirring. Fractional crystallization of the obtained dark-blue solution yielded, by slow evaporation in the air, few dark-blue crystals (**1t**) followed by a mixture of light-blue crystals of **1m$_4$** (one of which was employed for a SCXRD determination) and green needles of **1m$_2$**. From mother liquors, a pure fraction of **1m$_2$** was collected, washed with MeOH, and dried under vacuum.

1t: Anal. (%) Calcd for $Cu_3(OH)(pz)_3(Furc)_2(Hpz)(H_2O)$: C = 38.85; H = 3.09; N = 15.63. Found: C = 37.50; H = 2.97; N = 15.34. IR (ATR, cm^{-1}): 3130, 3094, 1598, 1583, 1557, 1478, 1407, 1388, 1364, 1281, 1223, 1189, 1179, 1141, 1063, 1027, 1011, 931, 885, 820, 783, 769, 750, 624.

1m$_2$: Yield: 660 mg, 50% (with respect to Cu). Anal. (%) Calcd for $Cu(Furc)_2(Hpz)_2$: C = 45.55; H = 3.35; N = 13.28. Found: C = 45.95; H = 3.42; N = 12.89. IR (ATR, cm^{-1}): 3137, 3107, 1577, 1541, 1478, 1406, 1366, 1232, 1188, 1076, 1019, 954, 931, 883, 861, 779, 752, 741, 649, 635, 618. μ_{eff} (296 K) = 2.01 μ_B (calculated for $C_{16}H_{14}CuN_4O_6$).

Reaction of $[Cu(Form)_2\cdot 4H_2O]$ + Hpz in H_2O. Synthesis of $[\{cis\text{-}Cu(Form)_2(Hpz)_2\}\{trans\text{-}Cu(Form)_2(Hpz)_2\}]$, ***2d****.* Hydrated copper(II) formate (5.0 g, 22 mmol) was dissolved in 45 mL of water, and Hpz (2.80 g, 41.1 mmol) dissolved in 15

https://doi.org/10.1021/acs.cgd.1c00861
Cryst. Growth Des. 2022, 22, 1032−1044

Table 1. Crystal Data and Structure Refinement for Compounds 1−3[a]

	1t	$1m_4$	$1m_2$	2d
exptl details	a, d	a, d	a, d	b
formula	$C_{22}H_{22}Cu_3N_8O_8$	$C_{22}H_{22}CuN_8O_6$	$C_{16}H_{14}CuN_4O_6$	$C_{16}H_{20}Cu_2N_8O_8$
FW, g mol^{-1}	717.09	558.03	421.86	579.48
crystal symmetry	triclinic	triclinic	triclinic	monoclinic
space group	$P\bar{1}$	$P\bar{1}$	$P\bar{1}$	$C2/c$
a, Å	7.1480(4)	7.9266(3)	5.3036(2)	13.2665(12)
b, Å	14.0279(11)	7.9453(3)	7.3358(3)	11.8611(12)
c, Å	14.0304(9)	11.0543(3)	11.8764(4)	13.9781(9)
α, deg	66.215(7)	72.926(3)	72.092(3)	90
β, deg	83.120(5)	69.066(3)	79.803(3)	91.709(1)
γ, deg	83.123(5)	72.686(3)	77.414(3)	90
cell volume, Å^3	1274.13(16)	606.93(4)	426.09(3)	2198.5(3)
Z	2	1	1	4
D_c, Mg m^{-3}	1.869	1.527	1.644	1.751
$F(000)$	722	287	215	1176
crystal size, mm	0.19 × 0.06 × 0.05	0.44 × 0.38 × 0.20	0.30 × 0.10 × 0.07	0.30 × 0.24 × 0.20
T, K	298(2)	298(2)	298(2)	298(2)
μ, mm^{-1} (λ)	2.547 (Mo Kα)	0.956 (Mo Kα)	1.325 (Mo Kα)	1.996 (Mo Kα)
θ limits, deg	1.6−29.9	2.0−32.0	1.8−31.9	2.3−28.5
refl collected	18204	15882	11073	9306
unique refl (R_{int})	6507 (0.0318)	3917 (0.0285)	2735 (0.0288)	2630 (0.0223)
GooF on F^2	1.155	1.076	1.051	1.137
$R_1(F)$[a], $wR_2(F^2)$[b]	0.0531, 0.1049	0.0335, 0.0881	0.0314, 0.0848	0.0247, 0.0647
largest diff. peak and hole, e Å^{-3}	0.45 and −0.51	0.52 and −0.32	0.49 and −0.25	0.23 and −0.46
	3h	3h′		3m
exptl details	c, d	p		a
formula	$C_{50}H_{56}Cu_6N_{12}O_{14}$	$C_{23}H_{20}Cu_3N_6O_5$		$C_{20}H_{18}CuN_4O_4$
FW, g mol^{-1}	1430.30	651.09		441.92
crystal symmetry	triclinic	triclinic		orthorhombic
Space group	$P\bar{1}$	$P\bar{1}$		$Pbcn$
a, Å	10.036(3)	9.9775(7)		21.495(2)
b, Å	11.249(2)	11.565(4)		9.3209(9)
c, Å	13.007(3)	12.303(4)		9.8193(10)
α, deg	87.045(18)	115.356(8)		90
β, deg	73.67(2)	89.210(7)		90
γ, deg	82.045(19)	94.040(4)		90
cell volume, Å^3	1395.5(6)	1279.55(10)		1967.3(3)
Z	1	2		4
D_c, Mg m^{-3}	1.702	1.690		1.492
$F(000)$	726	654		908
crystal size, mm	0.17 × 0.08 × 0.02	powder		0.20 × 0.10 × 0.09
T, K	173(2)	300(2)		297(2)
μ, mm^{-1} (λ)	2.320 (Mo Kα)	3.290 (Cu Kα)		1.145 (Mo Kα)
θ limits, deg	1.6−24.7	3.0−70.0		3.2−26.0
refl collected	7525	1109 refl, 2577 points		36496
unique refl (R_{int})	3973 (0.0902)	1109		1933 (0.0341)
GooF on F^2	1.135	7.478		1.202
$R_1(F)$[a], $wR_2(F^2)$[b]	0.0998, 0.2660	R_{Bragg} 0.033, $R(F^2)$ 0.069, R_{wp} 0.091, R_p 0.069, R_{exp} 0.012		0.0550, 0.1336
largest diff. peak and hole, e Å^{-3}	1.38 and −0.76	−		0.329 and −0.359

[a]Notes: a−p refer to the data collection, structure solution, and refinement details reported in the Supporting Information.

mL of water was added under stirring. The mixture was stirred for 2 h, and the obtained blue solid was filtered, washed with water, dried, and recognized as the previously reported species $[Cu_3(\mu_3\text{-OH})(\mu\text{-pz})_3(Form)_2(Hpz)_2]\cdot H_2O$, **A**.[28] Dark-blue mother liquors were allowed to evaporate, and fractional crystallization yielded two less pure fractions of **A** followed by a pure fraction of well-formed blue crystals of **2d**, which were collected, washed with cold water, and dried under vacuum.

2d. Yield: 1.425 g, 24% (with respect to Hpz). Anal. (%) Calcd for $\{Cu(Form)_2(Hpz)_2\}$: C = 33.16; H = 3.48; N = 19.34. Found: C = 33. 49; H, = 3.41; N = 18.95. IR (ATR, cm^{-1}): 3137, 3118, 3055, 2993, 1598, 1411, 1390, 1330, 1314, 1164, 1146, 1070, 1050, 945, 916, 903, 870, 843, 794, 768, 653, 612. μ_{eff} (293 K) = 2.79 μ_B (calculated for $C_{16}H_{20}Cu_2N_8O_8$).

Reaction of $[Cu(Bnz)_2(H_2O)_2\cdot H_2O]$ + Hpz in MeOH. Synthesis of $[\{Cu_3(\mu_3\text{-OH})(\mu\text{-pz})_3(Bnz)_2(MeOH)\}_2]\cdot 2MeOH$,

https://doi.org/10.1021/acs.cgd.1c00861
Cryst. Growth Des. 2022, 22, 1032−1044

Table 2. Structurally Characterized Derivatives Obtained from the Reaction of $Cu(RCOO)_2(H_2O)_x$ with Hpz

	mononuclear				
RCOO	$Cu(RCOO)_2(Hpz)_2$	$Cu(RCOO)_2(Hpz)_4$	dinuclear	trinuclear	hexanuclear
Furc	**1m$_2$** (1D CP)	**1m$_4$**		**1t**	
Form			**2d** (3D CP)		
Bnz	**3m**				**3h**, **3h′** (1D CP)

3h. A solution of Hpz (97 mg, 1.42 mmol) in 10 mL of MeOH was added to 332 mg (0.92 mmol) of $[Cu(Bnz)_2(H_2O)_2]\cdot H_2O$, partly dissolved in 200 mL of MeOH. The solid dissolved completely, and the slow evaporation in the air of the dark green-blue solution yielded blue crystals of **3h** that became rapidly gray by standing out of the mother liquors. Some crystals were maintained in the presence of MeOH and were employed to obtain a low-temperature (173 K) SCXRD structural determination. The remaining crystals were dried under vacuum, yielding a green-gray polycrystalline solid (**3h′**).

3h′. Yield: 80 mg, 43% (with respect to Cu). Anal. (%) Calcd for $Cu_3(OH)(pz)_3(Bnz)_2$: C = 42.43; H = 3.10; N = 12.91. Found: C = 42.73; H = 3.00; N = 12.71. IR (ATR, cm^{-1}): 3067, 1567, 1560, 1543, 1491, 1400, 1382, 1280, 1177, 1059. μ_{eff} (299 K) = 2.48 μ_B (calculated for $C_{38}H_{40}Cu_6N_{12}O_{10}$).

*Synthesis of [Cu(Bnz)$_2$(Hpz)$_2$], **3m***. From mother liquors of the synthesis of **3h**, some stable blue crystals of **3m** formed that were washed with a few drops of cold MeOH and dried under vacuum. By performing the reaction of $[Cu(Bnz)_2(H_2O)_2]\cdot H_2O$ with Hpz in 1:1 ratio, blue crystals of **3h** were the sole product, while by using a reaction ratio 1:4, it was possible to increase the yield of **3m**.

3m. Yield: 28% (with respect to Cu). Anal. (%) Calcd for $Cu(Bnz)_2(Hpz)_2$: C = 54.36; H = 4.11; N = 12.68. Found: C = 54.36; H = 4.12; N = 12.24. IR (ATR, cm^{-1}): 3286, 1599, 1517, 1467, 1370, 1253, 1167, 1113, 1065. μ_{eff} (291 K) = 1.84 μ_B (calculated for $C_{20}H_{18}CuN_4O_4$).

RESULTS

From the reactions of hydrated Cu^{II} 2-furancarboxylate, formate, and benzoate with Hpz in protic solvents two CPs based on mono- (**1m$_2$**) and dinuclear (**2d**) SBUs, as well as four mono- (**1m$_4$** and **3m**), tri- (**1t**), and hexanuclear (**3h**) species (Table 2) were isolated and structurally characterized. Moreover, the hexanuclear species **3h** easily loses coordinated and crystallized MeOH molecules, transforming, reversibly, into the **3h′** 1D CP (*vide infra*).

Structure Descriptions. The first product isolated from the reaction of copper(II) 2-furancarboxylate with Hpz consisted in few dark-blue crystals of compound $[Cu_3(\mu_3\text{-}OH)(\mu\text{-}pz)_3(Furc)_2(Hpz)]\cdot H_2O$, **1t**, which were employed to achieve a SCXRD structural characterization and an IR spectrum. The latter displays some absorption signals pertaining to the furancarboxylate ligands [$\nu_{as(COO)}$ and $\nu_{s(COO)}$, 1598 and 1487 cm^{-1}, respectively] suggesting, according to the Δ value,[56,57] a monodentate coordination mode. This feature is confirmed by the SCXRD determination showing the trinuclear triangular structure of **1t** (Figure 1), whose most relevant geometrical parameters fall in the ranges normally reported for this kind of compounds.[27−32,34,58−61]

In detail, the three Cu ions are placed in an almost equilateral triangular geometry through the coordination of N1−N6 pyrazolate nitrogens [Cu−N bond lengths range from 1.922(2) to 1.986(5) Å] and capping μ_3-O1 [Cu−O1 bond lengths range from 1.892(4) to 2.065(4) Å], which is placed out of the plane defined by the three Cu ions of *ca.* 0.42 Å. The coordination environment of the copper ions is completed by a pyrazole molecule coordinated to Cu3 [Cu3−N7 2.030(8) Å] and by two furancarboxylate ions bonded to Cu1 and Cu2. While a carboxylate anion coordinated to Cu1 acts as a monodentate ligand [Cu1−O2 1.968(3) Å], the second one asymmetrically chelates Cu2 by using carboxylate oxygen O5 and furan oxygen O7 [Cu2−O5 1.999(6), Cu2−O7 2.534(5) Å]. Thus, while the coordination geometry around Cu1 is almost exactly square planar (τ_4[62] = 0.07), in the case of Cu2 the square pyramidal geometry is slightly distorted (τ_5[63] = 0.07). Cu3 seemingly displays a strongly distorted square planar geometry (τ_4 = 0.37, τ'_4[64] = 0.34) due to the coordination of a neutral pyrazole molecule, besides nitrogens of pyrazolate ions and capping OH. Moreover, Cu1 is involved into a weak coordinative interaction with $O4^i$ of another symmetry-related trinuclear triangular unit [Cu1···$O4^i$ 2.856(3) Å, symmetry code i: 1 + *x*, *y*, *z*], thus the coordination geometry of Cu1 can be defined, approximatively, to be square pyramidal (τ_5 = 0.08). This weak bonding interaction is reinforced by a concomitant quite strong H-bond[65] involving the H atom of μ_3-OH and the uncoordinated furancarboxylate $O3^i$ atom of a symmetry-related trinuclear unit [O1···$O3^i$ 2.756(5) Å, O1−H10···$O3^i$ 160(5)°]. These two interactions contribute to generate 1D supramolecular chains, running parallel to the crystallographic *a* axis, as shown in Figure 2. In the same figure are also indicated other strong H-bonds connecting each trinuclear triangular cluster to the corresponding crystallization water molecule [O11···O6 2.719(8) Å, O11−H11B···O6 169(4)°].

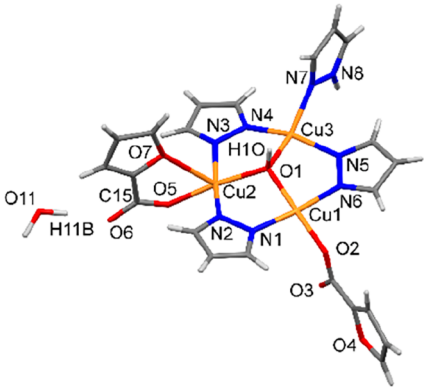

Figure 1. Trinuclear triangular molecular structure of **1t** with a partial atom labeling scheme.

Another strong H-bond[65] is relevant in the **1t** supramolecular structure. It involves NH moieties of coordinated pyrazoles and furancarboxylate oxygens $O6^{ii}$ belonging to symmetry-related trinuclear units [N8···$O6^{ii}$ 2.95(1) Å, N8−H8N···$O6^{ii}$ 165°, symmetry code ii: 1 − *x*, −*y*, −*z*], thus connecting two parallel supramolecular chains (Figure 3). The

https://doi.org/10.1021/acs.cgd.1c00861
Cryst. Growth Des. 2022, 22, 1032−1044

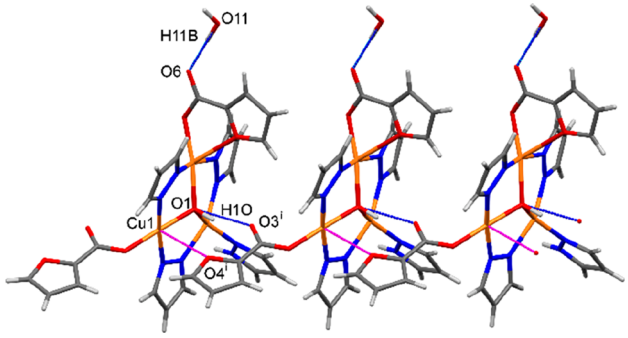

Figure 2. Supramolecular chain of **1t** formed by the weak coordinative interactions Cu1···O4^{i} (magenta dotted lines) and strong O1···O3^{i} and O6···O11 H-bonds (blue dotted lines).

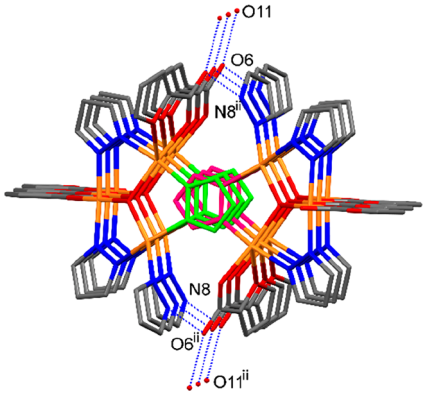

Figure 3. 1D supramolecular chains of **1t** connected by N8−H8N···O6^{ii} H-bonds (blue dotted lines). Pyrazolate rings possibly involved in $\pi-\pi$ interactions (see text) are evidenced by green and magenta colors. H atoms have been omitted for clarity.

connections between the chains are likely reinforced by possible $\pi-\pi$ interactions between homologous C4−C5−C6−N4−N3 pyrazolate rings which interdigitate and whose adjacent centroids lie about 3.18 Å apart. Finally, the crystal packing of **1t** is shown in Figure S1. All the other geometrical parameters of **1t** are quite normal[27−32,58−61] and can be retrieved from the CIF file supplied as Supporting Information.

From the mother liquors of **1t** a mixture of dark-blue crystals of $[Cu(Furc)_2(Hpz)_4]$, **1m$_4$**, and light-green needles of $[Cu(Furc)_2(Hpz)_2]$, **1m$_2$**, were obtained, followed by a pure crop of **1m$_2$**. A crystal of **1m$_4$** was employed for a SCXRD determination and its molecular structure is shown in Figure 4.

The copper ion lies on an inversion center and presents an elongated octahedral coordination geometry with four pyrazole nitrogens in a square plane [Cu1−N1 2.018(2), Cu1−N3 2.038(1) Å] while the two axial carboxylates are coordinated to Cu in a monodentate fashion [Cu1−O1 2.372(1) Å]. In compound **1m$_4$** strong "intramolecular" H-bonds[65] involving N4H4 and O2 carboxylate oxygen [N4···O2 2.697(2) Å, N4−H4···O2 172.0(1)°] are present and O2 is also involved into an "intermolecular" H-bond with N2H2 pyrazole system of a symmetry-related molecule [N2^{ii}···O2 2.814(2) Å, N2^{ii}−H2^{ii}···O2 142.9(1)°, symmetry code ii: $x-1, y, z$]. Incidentally, these H-bonds are likely responsible of the fairly symmetric electron delocalization in the O1−C7−O2 carboxylate moiety, revealed by the very similar C7−O1 and C7−O2 bond lengths [1.249(2) and 1.262(2) Å, respectively] (see Figure S2). More specifically, the strength of the supramolecular interactions

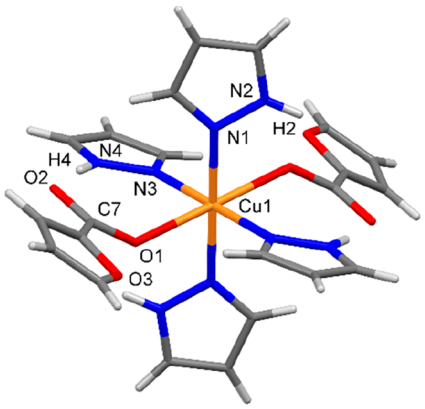

Figure 4. Molecular structure of **1m$_4$** with a partial atom labeling scheme.

involving O2 is overall comparable to the C7−O1 bonding interaction, thus favoring a balanced electron delocalization in the carboxylate moiety. The above-mentioned "intermolecular" H-bonds generate 1D supramolecular chains, one of which is shown in Figure S3. Finally, $\pi-\pi$ interactions between coordinated pyrazoles of these parallel chains (see Figure S4) generate 2D supramolecular networks, one of which is sketched in Figure S5.

From the mother liquors of the reaction of copper(II) 2-furancarboxylate with Hpz a pure crop of green needles of $[Cu(Furc)_2(Hpz)_2]$, **1m$_2$**, was also isolated. The molecular structure of compound **1m$_2$** (Figure 5) evidence structural

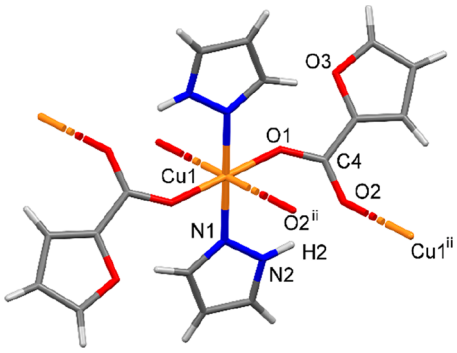

Figure 5. Molecular structure of **1m$_2$** with a partial atom labeling scheme.

features almost identical with those found in an analogous derivative previously obtained in the reaction of $Cu(Clac)_2$ with Hpz.[35] The copper ion, which lies on an inversion center, displays an octahedral geometry determined by the coordination of N1 [Cu1−N1 1.984(2) Å], O1 [Cu1−O1 1.993(1) Å], and O2 [Cu1−O2^{ii} 2.563(1) Å, symmetry code ii: $x-1, y, z$], the latter due to the *syn-anti* ditopic behavior of 2-furancarboxylate ions.

Thus, a 1D coordination polymer with $[Cu(Furc)_2(Hpz)_2]$ SBU forms based on chains constituted of subsequent 8-membered rings running parallel to the crystallographic *a* axis (Figure 6).

The formation of the eight membered rings is likely sustained by the presence of strong H-bonds[65] involving NH groups and O2 [N2···O2 2.710(2) Å, N2−H2···O2 161.8(1)°]. Other relevant supramolecular interactions are absent and parallel CPs generate the crystal packing shown in

https://doi.org/10.1021/acs.cgd.1c00861
Cryst. Growth Des. 2022, 22, 1032−1044

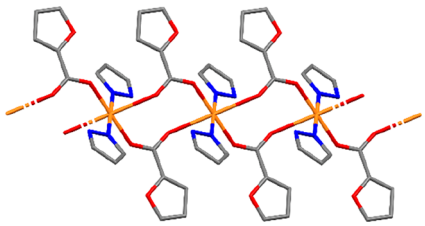

Figure 6. View down the crystallographic *b* axis of $\mathbf{1m_2}$ highlighting a part of a 1D CP formed through the self-assembly of $[Cu(Furc)_2(Hpz)_2]$ SBUs. H atoms have been omitted for sake of clarity.

Figure S6. The IR spectrum of $\mathbf{1m_2}$ in the region 1600−1300 cm^{-1} is in accordance with the bidentate bridging coordination mode of the furancarboxylate ion[66] evidenced by the SCXRD determination. A room temperature magnetic susceptibility measurement indicates that $\mathbf{1m_2}$ has a magnetic moment of 2.01 μ_B, as expected for magnetically noncoupled spins in copper(II) complexes.[67] Incidentally, this value is close to that of the reagent, $[Cu(Furc)_2(H_2O)_2]$ (1.98 μ_B).

Considering the relatively high pK_b value of the formate ion, we re-examined the reaction of copper formate with Hpz in water. Besides the already reported trinuclear species **A**,[28] obtained in a relatively low yield, a careful fractional crystallization of mother liquors led to the isolation of the species $[\{cis\text{-}Cu(Form)_2(Hpz)_2\}\{trans\text{-}Cu(Form)_2(Hpz)_2\}]$, **2d**, whose structure is shown in Figure 7.

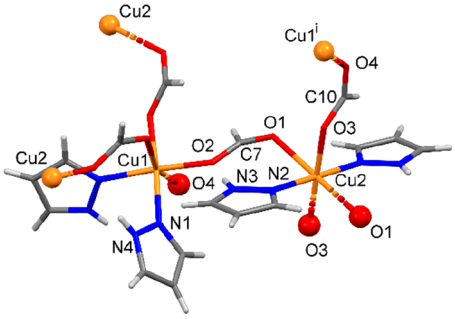

Figure 7. Molecular structure of **2d** with a partial atom labeling scheme.

The molecular structure of **2d** is characterized by the presence of two kinds of alternating Cu nodes having the same stoichiometry but different coordination geometries. Both Cu ions are indeed octahedrally coordinated by four O atoms from bridging formate anions and two N atoms belonging to monodentate Hpz molecules. The geometrical isomerism is given by the Hpz molecules which bind Cu1 in a *cis* fashion and Cu2 in a *trans* fashion. Thus, while Cu2 lies on an inversion center, Cu1 is crossed by a 2-fold axis. All formate ions act as bridging *syn*−*anti* linkers generating a 3D CP. In Figure 7, the Cu and O atoms represented with the ball-and-stick style indicate the nodes from where the polymer grows. In detail, Cu1 and Cu2 are connected through the O2−C7−O1 [Cu1−O2 1.968(1), Cu2−O1 2.512(2) Å] and O3−C10−O4 [Cu2−O3 1.964(1), $Cu1^i$−O4 2.411(2) Å] carboxylate moieties, thus generating 16- and 32-membered macrocycles which are the bricks of parallel undulating 2D CPs, one of which is partly depicted in Figure 8.

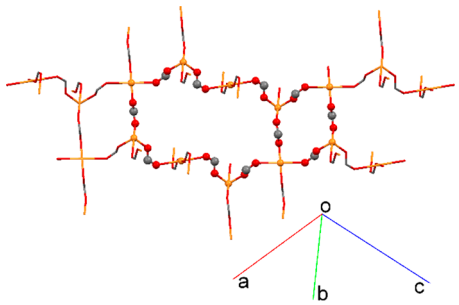

Figure 8. Compound **2d**. 32- and 16-membered macrocycles (ball-and-stick representation) generating an undulating sheet. Coordinated pyrazole molecules and H atoms have been omitted for sake of clarity.

On the other hand, these parallel wavy sheets are further joined together through other, almost perpendicular, macrocycles, thus forming the 3D cages shown in Figure 9.

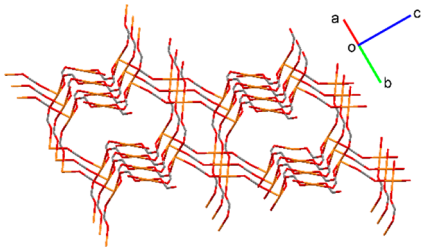

Figure 9. 3D cages in compound **2d**. Coordinated pyrazole molecules and H atoms have been omitted for sake of clarity.

A series of strong H-bonds[65] involving pyrazole NH groups and O2 and O3 formate oxygens (see Figure S7) likely reinforce the 3D assembly of **2d**.

The bridging based on *syn*−*anti* coordination of the formate anions is also confirmed by the IR spectrum data of **2d**: main signals are observed at 1314 cm^{-1}, with a shoulder at 1330 cm^{-1} and a broader absorption at 1598 cm^{-1}, that can be tentatively assigned to the ν_s(COO) symmetric stretching, C−H rocking and ν_{as}(COO) asymmetric stretching modes, respectively; the large Δ value (284 cm^{-1}) confirms the asymmetric bidentate bridging coordination.[68] The magnetic susceptibility value calculated for the dinuclear **2d** species (2.79 μ_B) is in the range expected for two unpaired electrons, thus suggesting the absence of magnetic interactions between Cu1 and Cu2.

The reaction of copper(II) benzoate with Hpz (*ca.* 1:1.5 molar ratio) in MeOH led to the isolation of deep blue crystals of the hexanuclear derivative $[\{Cu_3(\mu_3\text{-}OH)(\mu\text{-}pz)_3(Bnz)_2(MeOH)\}_2]\cdot 2MeOH$, **3h**, that are unstable in the air. Thus, the molecular structure of **3h** (Figure 10) was determined by carrying out a low-temperature (173 K) SCXRD measurement on a MeOH soaked crystal covered with mineral oil.

The coordination schemes of copper ions are determined, besides the pyrazolates nitrogens [Cu1−N6 1.93(1), Cu1−N1 1.90(1), Cu2−N2 1.90(2), Cu2−N3 1.88(2), Cu3−N4 1.92(2), Cu3−N5 1.95(2) Å] and capping μ_3-O1 [Cu1−O1 2.00(1), Cu2−O1 1.98(1), Cu3−O1 1.96(1) Å], by carboxylates oxygens O2, O4, and O5 and methanol O6. As a result, Cu1 displays a square planar coordination geometry (τ_4 = 0.04), analogously to Cu3 (τ_4 = 0.06), where a weak chelating interaction of O5 is also present [Cu3−O4 1.98(1),

https://doi.org/10.1021/acs.cgd.1c00861
Cryst. Growth Des. 2022, 22, 1032−1044

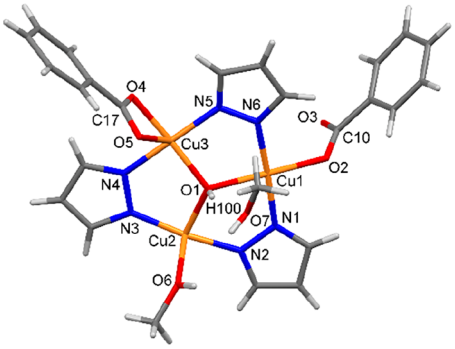

Figure 10. Triangular trinuclear asymmetric unit of **3h** with a partial atom labeling scheme.

Cu3−O5 2.59(1) Å]. The square pyramidal coordination geometry of Cu2 (τ_5 = 0.08), to which a methanol molecule is axially bonded, is completely described taking into account that the "true" molecular structure of **3h** corresponds to a hexanuclear system, generated by the almost symmetric *syn-syn* bridging coordination of the O2−C10−O3 carboxylate joining Cu1 to Cu2^{i} of the symmetry-related trinuclear unit [Cu1−O2 1.95(1), Cu2^{i}−O3 1.99(1) Å, symmetry code i: $-x$, $1-y$, $-z$] (Figure 11).

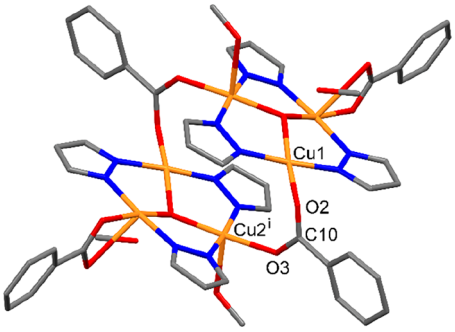

Figure 11. Hexanuclear assembly of **3h**. H atoms and crystallization methanol molecules have been omitted for clarity.

Analogously to what observed in other strictly related trinuclear triangular Cu^{II} derivatives, O1 is placed out of the plane defined by the three Cu ions of *ca.* 0.42 Å. All the other geometrical parameters are quite normal for this kind of compounds.[27−32,34,58−61] A relevant feature in the overall structure of **3h** is the presence of three kinds of H-bonds, involving crystallization and coordinated methanol molecules, [O1···O7 2.61(2) Å, O1−H100···O7 148(12)°, O6^{ii}···O5 2.72(2) Å, O6^{ii}−H6A^{ii}···O5 163°, O7^{ii}···O5 2.70(2) Å, O7^{ii}−H7A^{ii}···O5 158° symmetry code ii: $-x$, $-y$, $-z$] that, acting as bridges, join the hexanuclear clusters and generate 1D supramolecular columns, one of which is partly depicted in Figure 12. These assemblies, running parallel to the crystallographic *b* axis, further arrange in the crystal packing of **3h**, as shown in Figure S8.

These H-bonds likely play a crucial role in the overall stability of **3h** and its methanol sorption−desorption behavior. In effect, by standing in the air the blue crystals of **3h** quickly transform into a gray-green polycrystalline powder (**3h′**) whose elemental analysis fits quite well with the formulation $Cu_3(OH)(pz)_3(Bnz)_2$. Moreover, the crystal structure of **3h′**, solved by PXRD (see Figure S9), confirms that **3h** has lost both coordinated and crystallization MeOH molecules (Figure 13), while the coordination geometry of Cu1 and Cu3 remains almost unchanged. Cu1 displays a square planar coordination

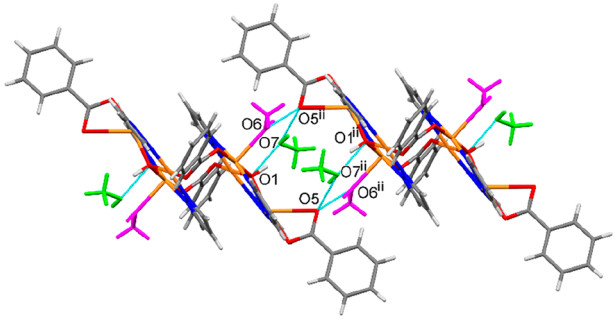

Figure 12. Supramolecular assembly of the hexanuclear moieties of **3h**, driven by H-bonds (light-blue dotted lines) and involving coordinated and crystallization MeOH molecules evidenced with magenta and green color, respectively.

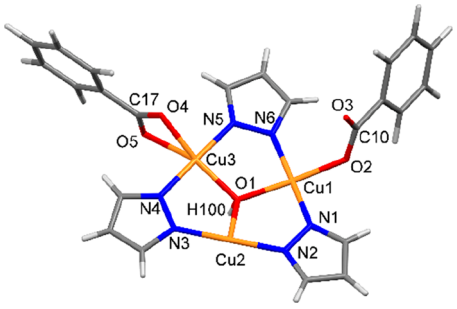

Figure 13. Trinuclear asymmetric unit of **3h′** with a partial atom labeling scheme.

geometry determined, besides capping μ_3-O1, by N1, N6, and O2 [Cu1−O2 1.985(4) Å], and similarly, Cu3 is coordinated by N4, N5, and O4, [Cu3−O4 1.948(4) Å] and, additionally, weakly interacts with O5 [Cu3−O5 2.672(4)].

Analogously to **3h**, also in the case of **3h′** the "true" molecular structure consists in a hexanuclear system, generated through the *syn−syn* coordination of O2−C10−O3 carboxylate bridging Cu1 to Cu2^{i} of a symmetry-related trinuclear unit (see Figure 14).

These hexanuclear clusters are further connected to each other thanks to the *syn-anti* ditopic behavior of O5

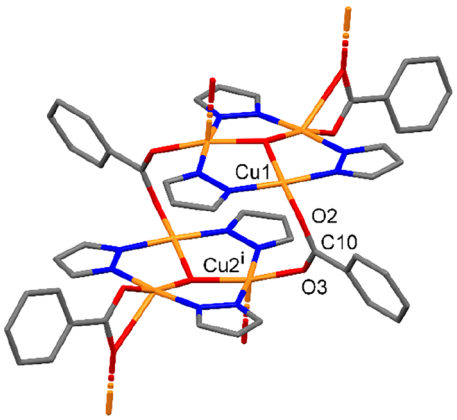

Figure 14. Hexanuclear assembly of **3h′**. H atoms have been omitted for clarity.

https://doi.org/10.1021/acs.cgd.1c00861
Cryst. Growth Des. 2022, 22, 1032−1044

coordinating, besides Cu3, also Cu2 of a symmetry-related hexanuclear system [Cu2^{ii}−O5 2.045(4) Å], thus generating 1D CPs running parallel to the crystallographic *a* axis (Figure 15).

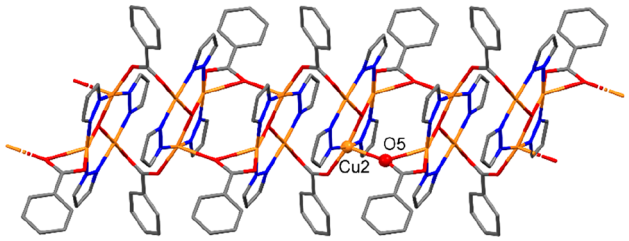

Figure 15. View of **3h′** evidencing a part of a 1D CP formed through the connection of hexanuclear clusters. H atoms have been omitted for clarity.

In Figure 16 are shown the most relevant differences between the 1D supramolecular assembly of **3h** and the 1D CP of **3h′**. It appears evident that the presence of coordinated and crystallization MeOH molecules, on one hand makes possible the formation of the 1D supramolecular chain, but contributes to maintain the distance between the two hexanuclear systems at a value of about 11 Å. When crystallization and coordinated MeOH molecules are removed from **3h**, the benzoate oxygen O5 can quite strongly coordinate to the nearby unsaturated Cu2 ion pertaining to another hexanuclear cluster and the two systems can approach each other at a distance of about 10 Å.

Due to the rapid release of methanol from **3h**, it was possible to obtain the FT-IR spectrum of **3h′** only. It exhibits two different signals for the symmetric and antisymmetric COO stretching, the Δ values being 167 and 178 cm^{-1} which are in accordance with a symmetric bridging coordination and chelating bidentate coordination modes for arylcarboxylates.[69,70] The magnetic moment measured for the same compound (2.49 μ_B) is close to the value reported, for example, for trinuclear triangular copper(II) succinate complexes and also supports the occurrence of metal−metal interactions in magnetically coupled spin-only species.[44]

By carrying out the synthesis of **3h** with an excess of Hpz, it was possible to crystallize, from mother liquors, the mononuclear derivative [Cu(Bnz)$_2$(Hpz)$_2$], **3m**, whose molecular structure is shown in Figure 17.

Copper ion, which is placed on an inversion center, displays a square planar coordination geometry determined by N1 [Cu1−N1 1.977(3) Å] and O1, [Cu1−O1 1.942(3) Å], which is expanded by a weak chelating interaction with O2 [Cu1−O2 2.676(3) Å]. Finally, intermolecular H-bonds involving the N2H2 group and O2 pertaining to another symmetry-related molecule [N2···O2^{ii} 2.792(4) Å, N2−H2···O2^{ii} 142.7(3)°, symmetry code ii: x, $-y + 1$, $z - {}^1/_2$] (Figure S10) likely contribute to the overall formation of the crystal packing of **3m** (Figure S11).

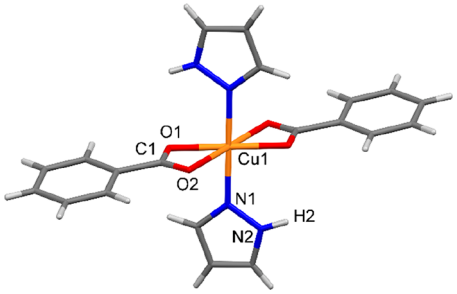

Figure 17. Molecular structure of **3m** with a partial atom labeling scheme.

The magnetic moment (1.84 μ_B) determined for **3m** is in the range reported for benzoate complexes showing magnetically isolated copper(II) centers.[67,71]

DISCUSSION

Influence of the Carboxylate Basicity. Thanks to the ability of monocarboxylates to coordinate more than one metal ion, mono and three-dimensional CPs, besides mono- and trinuclear copper(II) derivatives, have been synthesized. Moreover, our results confirm the hypothesis that the basicity of carboxylate ions plays a determinant role in directing the reaction, in protic solvents, of copper(II) carboxylates with pyrazole toward the formation of mononuclear [Cu(RCOO)$_2$(Hpz)$_n$] (n = 2 or 4) or trinuclear triangular [Cu$_3$(μ_3-OH)(μ-pz)$_3$(RCOO)$_2$] species. To obtain the trinuclear triangular [Cu$_3$(μ_3-OH)(μ-pz)$_3$]$^{2+}$ moiety, water and pyrazole need to be deprotonated, giving sufficient concentrations of OH$^-$ and pz$^-$ anions. When the deprotonating agent is the carboxylate ion, only pK_b values lower than *ca.* 9.7[34] lead to the exclusive formation of the trinuclear clusters. Carboxylates having higher pK_b values, as in the case of copper trifluoroacetate (pK_b = 13.48),[27] are unable to efficiently deprotonate water and/or Hpz; thus, the reactions generate only mononuclear derivatives coordinating neutral Hpz. With carboxylates having intermediate pK_b values both mono and trinuclear systems form, as evidenced in the case of chloroacetate[35] and in the present work. Moreover, in the reactions of copper carboxylates having intermediate pK_b

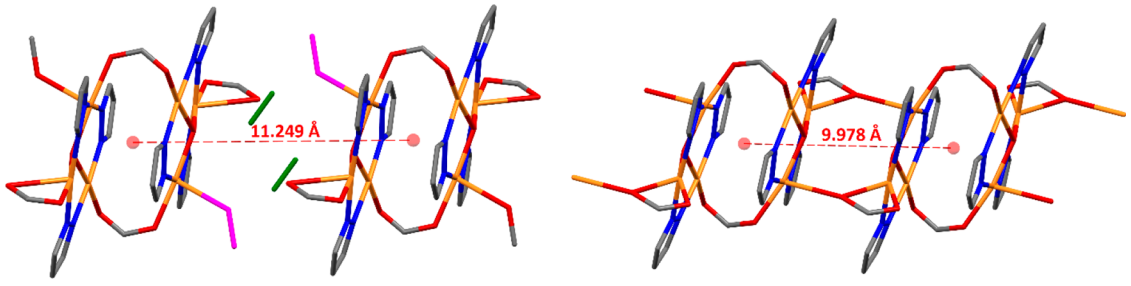

Figure 16. Comparison between the view of two adjacent hexanuclear clusters in **3h** (left), where coordinated and crystallization MeOH molecules are evidenced in magenta and green color, respectively, and the 1D structure of **3h′** (right). H atoms and phenyl rings have been omitted for clarity. Transparent red balls show the centers of the hexanuclear clusters.

https://doi.org/10.1021/acs.cgd.1c00861
Cryst. Growth Des. 2022, 22, 1032−1044

values also the Cu/Hpz ratio is a relevant item, with low ratios favoring the formation of mononuclear derivatives.

Structural Features. The systems synthesized in this work include mononuclear discrete complexes $\mathbf{1m}_4$ and **3m** and the 1D CP $\mathbf{1m}_2$. The latter shows a structure analogous to that of the previously reported $[Cu(Clac)_2(Hpz)_2]$ derivative.[35] The rather peculiar 3D structure of **2d** CP originates from the alternation of two kinds of Cu nodes with the same stoichiometry but different coordination geometries. Each Cu is coordinated by two monodentate ligands (Hpz) and four bidentate ligands ($HCOO^-$), but the monodentate ligands bind Cu1 in a *cis* fashion and Cu2 in a *trans* fashion. Consequently, Cu1 connectors are distorted tetrahedra (namely a "quarters of a tetrahedron") and Cu2 are square planar connectors. The assembly of tetrahedral and square planar nodes in 1:1 ratio forms a distorted **pts** net (Figure 18).[72]

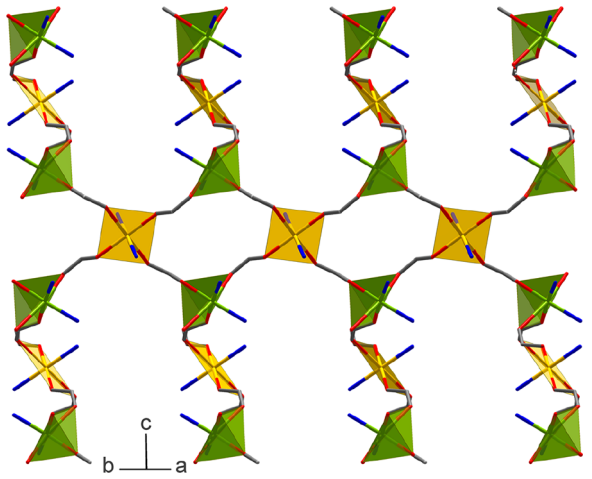

Figure 18. Simplified representation of the 3D network of **2d**, with emphasis on the geometry of the Cu nodes. Cu1 centers are represented as green distorted tetrahedra, while Cu2 sites are represented as yellow squares, and both are decorated by monotopic HPz ligands, simplified as blue atoms. The square nodes assume orientations parallel and perpendicular to the plane of the figure, and are connected to the tethahedral nodes via *syn*−*anti* formate bridges, represented in gray, to form a 3D network.

Compounds **1t**, **3h**, and **3h′**, based on the $[Cu_3(\mu_3\text{-}OH)(\mu\text{-}pz)_3]^{2+}$ moiety, evidence interesting structural features. Compound **1t** represents a quite rare case of isolated trinuclear system, this feature having been previously found only in two derivatives obtained in the reaction of copper propanoate with Hpz in water.[29] The hexanuclear structures of **3h** and **3h′** display a 1D-like supramolecular self-assembly which is recurrent for trinuclear systems coordinated by carboxylates with similar steric hindrance. In this context, it has been recently reported the synthesis of compound $[\{Cu_3(\mu_3\text{-}OH)(\mu\text{-}pz)_3(Bnz)_2(EtOH)\}_2]\cdot 2EtOH$, **B**,[73] whose structure differs from that of **3h** only by the presence of coordinated and crystallized EtOH molecules instead of MeOH. This closely related compound has been obtained as light-blue crystals through a microwave-assisted reaction of copper chloride with sodium benzoate and Hpz at 373 K in EtOH/water mixture, followed by slow evaporation of the solvent. There is no mention about its stability in absence of solvent, even though the XRD data performed at 100 K may indicate its instability at room temperature. The scenario where this material, contrary to the behavior observed for **3h**, did not lose solvent molecules could be explained by the lower volatility of EtOH with respect to MeOH. Finally, it is noteworthy that the 1D CP structure of **3h′** is very similar to those found in the methacrylate (Methacr) and *cyclo*-hexylcarboxylate (c-Hexc) trinuclear derivatives $[\{Cu_3(\mu_3\text{-}OH)(\mu\text{-}pz)_3(Methacr)_2\}_2]$[31] and $[\{Cu_3(\mu_3\text{-}OH)(\mu\text{-}pz)_3(c\text{-}Hexc)_2\}_2]$,[34] respectively, as shown in Figure S12.

Sorption−Desorption Behavior of 3h/3h′. The loss of crystallization and coordinated MeOH molecules of **3h** makes possible the aggregation of the hexanuclear clusters transforming a H-bond based 1D network into a 1D CP, and this process is reversible. As a matter of fact, at ambient conditions, **3h** rapidly loses MeOH to form **3h′**, as evidenced by the disaggregation of the single crystals accompanied by a change of color from blue to gray-green. However, the resulting powder became quickly blue when soaked with MeOH, and the drying-soaking process can be repeated, suggesting the possibility that reversible MeOH sorption−desorption processes are operating. To understand this behavior, we performed a PXRD study on compound **3h** in different conditions (Figure 19).

First, **3h** was sealed with MeOH into a capillary, and its PXRD pattern was found to be consistent with the one simulated from the single-crystal structural model (Figure S13). The capillary was then opened and PXRD patterns were measured again over 1 week. The desolvation was observed as gradual disappearance of the diffraction peaks of **3h** and appearance of new ones (Figure S14). Within ca. 2 days, **3h** completely transforms into an intermediate phase which could not be characterized satisfactorily. **3h′** peaks start appearing afterward, as the product of a second slower transformation. The formation of intermediate phases could suggest that the loss of MeOH occurs stepwise, likely involving the loss of crystallization molecules first and of the coordinated ones last. Finally, the same sample was analyzed again after being exposed to the air for 1 week, yielding the pattern of pure **3h′**, which could be indexed with a triclinic unit cell, and used for structure solution and refinement. The same capillary was then refilled with MeOH and sealed, and its pattern confirmed the quantitative restoration of solvated **3h** in one step.

CONCLUSIONS

In this study, we have reported the synthesis and structures of new coordination compounds of Cu^{II} and pyrazole with 2-furancarboxylate, formate, and benzoate under room conditions in protic solvents. The concentration of reagents and the specific protic solvent contribute to modulating the amount of mononuclear and higher nuclearity species by tuning the pH of the solution and to the intricate interplay of complexation equilibria. However, positioning these results within the extended library of coordination compounds assembled by Cu^{II}, Hpz/pz and $RCOO^-$ allowed us to rationalize the formation of mono-/dinuclear Cu species featuring neutral Hpz ligands vs tri-/hexanuclear species containing the triangular $[Cu_3(\mu_3\text{-}OH)(\mu\text{-}pz)_3]^{2+}$ cores as a function of the carboxylate basicity. The higher base strength promotes the deprotonation of Hpz and H_2O and turns them into ancillary ligands, allowing the formation of structural SBUs with high nuclearity. As a result the pK_b of carboxylate linkers appears to play a key role in driving the formation of trinuclear moieties over lower nuclearity nodes. This parameter

https://doi.org/10.1021/acs.cgd.1c00861
Cryst. Growth Des. 2022, 22, 1032−1044

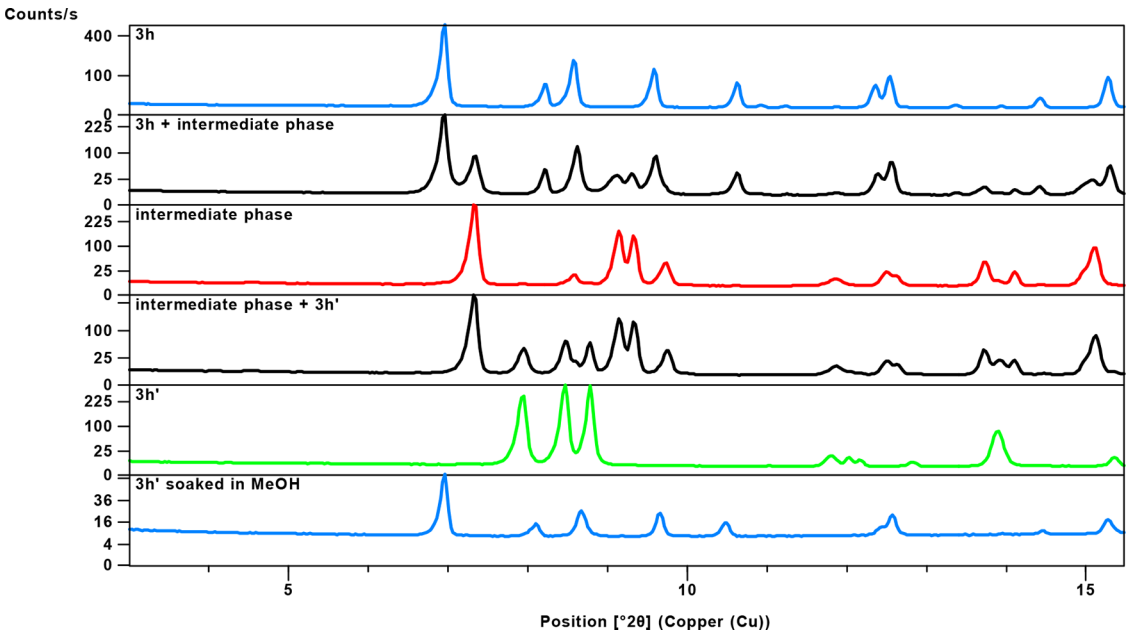

Figure 19. PXRD diffractograms of **3h**/**3h′** carried out in the presence of MeOH (at the top) and during the desorption experiment. Finally, the bottom pattern was obtained after reabsorption of MeOH.

can be used as a simple concept to inform the design of materials based on the broadly used building blocks Cu^{II}, Hpz/pz, and $RCOO^-$ and will help to harness the versatility of this ternary system.

■ ASSOCIATED CONTENT

Supporting Information

The Supporting Information is available free of charge at https://pubs.acs.org/doi/10.1021/acs.cgd.1c00861.

X-ray diffraction instrumental details, data collectionm and data reduction, structure solution and refinement, and Figures S1−S14 (PDF)

Accession Codes

CCDC 2098579−2098585 contain the supplementary crystallographic data for this paper. These data can be obtained free of charge via www.ccdc.cam.ac.uk/data_request/cif, or by emailing data_request@ccdc.cam.ac.uk, or by contacting The Cambridge Crystallographic Data Centre, 12 Union Road, Cambridge CB2 1EZ, UK; fax: +44 1223 336033.

■ AUTHOR INFORMATION

Corresponding Authors

Rebecca Scatena − *Dipartimento di Scienze Chimiche, University of Padova, I-35131 Padova, Italy; Department of Physics, Clarendon Laboratory, University of Oxford, Oxford OX1 3PU, U.K.;* orcid.org/0000-0002-3500-1455; Email: rebecca.scaten@physics.ox.ac.uk

Luciano Pandolfo − *Dipartimento di Scienze Chimiche, University of Padova, I-35131 Padova, Italy*; Email: luciano.pandolfo@unipd.it

Magda Monari − *Dipartimento di Chimica "G. Ciamician", University of Bologna, I-40126 Bologna, Italy*; Email: magda.monari@unibo.it

Authors

Sara Massignani − *Dipartimento di Scienze Chimiche, University of Padova, I-35131 Padova, Italy*

Arianna E. Lanza − *Center for Nanotechnology Innovation @ NEST, Istituto Italiano di Tecnologia, 56127 Pisa, Italy;* orcid.org/0000-0002-7820-907X

Federico Zorzi − *Dipartimento di Geoscienze, University of Padova, I-35131 Padova, Italy*

Fabrizio Nestola − *Dipartimento di Geoscienze, University of Padova, I-35131 Padova, Italy*

Claudio Pettinari − *Scuola di Farmacia, University of Camerino, I-62032 Camerino (MC), Italy;* orcid.org/0000-0002-2547-7206

Complete contact information is available at: https://pubs.acs.org/10.1021/acs.cgd.1c00861

Notes

The authors declare no competing financial interest.

■ ACKNOWLEDGMENTS

The authors acknowledge Prof. Piero Macchi for kindly providing access to low-temperature SCXRD measurement. M.M. gratefully acknowledges the University of Bologna for financial support. C.P. acknowledges support from the University of Camerino.

■ REFERENCES

(1) Férey, G.; Serre, C. Large breathing effects in three-dimensional porous hybrid matter: facts, analyses, rules and consequences. *Chem. Soc. Rev.* **2009**, *38*, 1380−1399.

(2) Lu, W.; Wei, Z.; Gu, Z.-Y.; Liu, T.-F.; Park, J.; Park, J.; Tian, J.; Zhang, M.; Zhang, Q.; Gentle, T., III; Bosch, M.; Zhou, H.-C. Tuning the structure and function of metal−organic frameworks via linker design. *Chem. Soc. Rev.* **2014**, *43*, 5561−5593.

(3) Schneemann, A.; Bon, V.; Schwedler, I.; Senkovska, I.; Kaskel, S.; Fischer, R. A. Flexible metal−organic frameworks. *Chem. Soc. Rev.* **2014**, *43*, 6062−6096.

(4) Moulton, B.; Zaworotko, M. J. From Molecules to Crystal Engineering: Supramolecular Isomerism and Polymorphism in Network Solids. *Chem. Rev.* **2001**, *101*, 1629−1658.

(5) Mínguez Espallargas, G.; Coronado, E. Magnetic Functionalities in MOFs: From the Framework to the Pore. *Chem. Soc. Rev.* **2018**, *47*, 533−557.
(6) Perry, J. J., IV; Perman, J. A.; Zaworotko, M. J. Design and synthesis of metal−organic frameworks using metal−organic polyhedra as supermolecular building blocks. *Chem. Soc. Rev.* **2009**, *38*, 1400−1417.
(7) O'Keeffe, M.; Yaghi, O. M. Deconstructing the Crystal Structures of Metal−Organic Frameworks and Related Materials into Their Underlying Nets. *Chem. Rev.* **2012**, *112*, 675−702.
(8) Karmakar, A.; Titi, H. M.; Goldberg, I. Coordination Polymers of 5-(2-Amino/Acetamido-4-carboxyphenoxy)-benzene-1,3-dioic Acids with Transition Metal Ions: Synthesis, Structure, and Catalytic Activity. *Cryst. Growth Des.* **2011**, *11*, 2621−2636.
(9) Cook, Y. R.; Zheng, Y.-R.; Stang, P. J. Metal−Organic Frameworks and Self-Assembled Supramolecular Coordination Complexes: Comparing and Contrasting the Design, Synthesis, and Functionality of Metal−Organic Materials. *Chem. Rev.* **2013**, *113*, 734−777.
(10) Zhang, Z.; Zaworotko, M. J. Template-directed synthesis of metal−organic materials. *Chem. Soc. Rev.* **2014**, *43*, 5444−5455.
(11) Guillerm, V.; Kim, D.; Eubank, J. F.; Luebke, R.; Liu, X.; Adil, K.; Lah, M. S.; Eddaoudi, M. A supermolecular building approach for the design and construction of metal−organic frameworks. *Chem. Soc. Rev.* **2014**, *43*, 6141−6172.
(12) Tatikonda, R.; Bulatov, E.; Kalenius, E.; Haukka, M. Construction of Coordination Polymers from Semirigid Ditopic 2,2′-Biimidazole Derivatives: Synthesis, Crystal Structures, and Characterization. *Cryst. Growth Des.* **2017**, *17*, 5918−5926.
(13) Uemura, K. Syntheses and crystal structures of novel silver(I) coordination polymers based on linear or tetrahedral coordination environments. *Inorg. Chem. Commun.* **2008**, *11*, 741−744.
(14) Masciocchi, N.; Galli, S.; Sironi, A. X-ray powder diffraction characterization of polymeric metal diazolates. *Comments Inorg. Chem.* **2005**, *26*, 1−37.
(15) Zhang, J. P.; Chen, X. M. Crystal engineering of binary metal imidazolate and triazolate frameworks. *Chem. Commun.* **2006**, 1689−1699.
(16) Klingele, J.; Dechert, S.; Meyer, F. Polynuclear transition metal complexes of metal···metal-bridging compartmental pyrazolate ligands. *Coord. Chem. Rev.* **2009**, *253*, 2698−2741.
(17) Phan, A.; Doonan, C. J.; Uribe-Romo, F. J.; Knobler, C. B.; O'Keeffe, M.; Yaghi, O. M. Synthesis, Structure, and Carbon Dioxide Capture Properties of Zeolitic Imidazolate Frameworks. *Acc. Chem. Res.* **2010**, *43*, 58−67.
(18) Mohamed, A. A. Advances in the coordination chemistry of nitrogen ligand complexes of coinage metals. *Coord. Chem. Rev.* **2010**, *254*, 1918−1947.
(19) Olguin, J.; Brooker, S. Spin crossover active iron(II) complexes of selected pyrazole-pyridine/pyrazine ligands. *Coord. Chem. Rev.* **2011**, *255*, 203−240.
(20) Ouellette, W.; Jones, S.; Zubieta, J. Solid state coordination chemistry of metal-1,2,4-triazolates and the related metal-4-pyridyltetrazolates. *CrystEngComm* **2011**, *13*, 4457−4485.
(21) Aromi, G.; Barrios, l. A.; Roubeau, O.; Gamez, P. Triazoles and tetrazoles: Prime ligands to generate remarkable coordination materials. *Coord. Chem. Rev.* **2011**, *255*, 485−546.
(22) Zhang, J. P.; Zhang, Y. B.; Lin, J. B.; Chen, X. M. Metal Azolate Frameworks: From Crystal Engineering to Functional Materials. *Chem. Rev.* **2012**, *112*, 1001−1033.
(23) Cingolani, A.; Galli, S.; Masciocchi, N.; Pandolfo, L.; Pettinari, C.; Sironi, A. Sorption−Desorption Behavior of Bispyrazolato−Copper(II) 1D Coordination Polymers. *J. Am. Chem. Soc.* **2005**, *127*, 6144−6145.
(24) Bencini, A.; Casarin, M.; Forrer, D.; Franco, L.; Garau, F.; Masciocchi, N.; Pandolfo, L.; Pettinari, C.; Ruzzi, M.; Vittadini, A. Magnetic Properties and Vapochromic Reversible Guest-Induced Transformation in a Bispyrazolato Copper(II) Polymer: an Experimental and Dispersion-Corrected Density Functional Theory Study. *Inorg. Chem.* **2009**, *48*, 4044−4051.
(25) Casarin, M.; Forrer, D.; Pandolfo, L.; Pettinari, C.; Vittadini, A. Vapochromic properties versus metal ion coordination of β-bispyrazolato−copper(II) coordination polymers: a first-principles investigation. *CrystEngComm* **2015**, *17*, 407−411.
(26) Barbour, J. L. Crystal porosity and the burden of proof. *Chem. Commun.* **2006**, 1163−1168.
(27) Casarin, M.; Corvaja, C.; Di Nicola, C.; Falcomer, D.; Franco, L.; Monari, M.; Pandolfo, L.; Pettinari, C.; Piccinelli, F.; Tagliatesta, P. Spontaneous Self-Assembly of an Unsymmetric Trinuclear Triangular Copper(II) Pyrazolate Complex, [Cu3(μ3-OH)(μ-pz)3-(MeCOO)2(Hpz)] (Hpz = Pyrazole). Synthesis, Experimental and Theoretical Characterization, Reactivity, and Catalytic Activity. *Inorg. Chem.* **2004**, *43*, 5865−5876.
(28) Casarin, M.; Corvaja, C.; Di Nicola, C.; Falcomer, D.; Franco, L.; Monari, M.; Pandolfo, L.; Pettinari, C.; Piccinelli, F. One-Dimensional and Two-Dimensional Coordination Polymers from Self-Assembling of Trinuclear Triangular Cu(II) Secondary Building Units. *Inorg. Chem.* **2005**, *44*, 6265−6276.
(29) Di Nicola, C.; Karabach, Y. Yu; Kirillov, A. M.; Monari, M.; Pandolfo, L.; Pettinari, C.; Pombeiro, A. J. L. Supramolecular Assemblies of Trinuclear Triangular Copper(II) Secondary Building Units through Hydrogen Bonds. Generation of Different Metal−Organic Frameworks, Valuable Catalysts for Peroxidative Oxidation of Alkanes. *Inorg. Chem.* **2007**, *46*, 221−230.
(30) Di Nicola, C.; Garau, F.; Karabach, Y. Y.; Martins, L. M. D. R. S.; Monari, M.; Pandolfo, L.; Pettinari, C.; Pombeiro, A. J. L. Trinuclear Triangular Copper(II) Clusters − Synthesis, Electrochemical Studies and Catalytic Peroxidative Oxidation of Cycloalkanes. *Eur. J. Inorg. Chem.* **2009**, *2009*, 666−676.
(31) Contaldi, S.; Di Nicola, C.; Garau, F.; Karabach, Y. Y.; Martins, L. M. D. R. S.; Monari, M.; Pandolfo, L.; Pettinari, C.; Pombeiro, A. J. L. New coordination polymers based on the triangular [Cu3(μ3-OH)(μ-pz)3]2+ unit and unsaturated carboxylates. *Dalton Trans.* **2009**, 4928−4941.
(32) Pandolfo, L.; Pettinari, C. Trinuclear copper(II) pyrazolate compounds: a long story of serendipitous discoveries and rational design. *CrystEngComm* **2017**, *19*, 1701−1720.
(33) Carlotto, S.; Pandolfo, L.; Casarin, M. Trinuclear Cu(II) complexes from the classic [Cu2(RCOO)4(H2O)2] lantern complex and pyrazole: a DFT modelling of the reaction path. *Inorg. Chim. Acta* **2018**, *470*, 93−99.
(34) Massignani, S.; Scatena, R.; Lanza, A.; Monari, M.; Condello, F.; Nestola, F.; Pettinari, C.; Zorzi, F.; Pandolfo, L. Coordination polymers from mild condition reactions of copper(II) carboxylates with pyrazole (Hpz). Influence of carboxylate basicity on the self-assembly of the [Cu3(μ3-OH)(μ-pz)3]2+ secondary building unit. *Inorg. Chim. Acta* **2017**, *455*, 618−626.
(35) Carlotto, S.; Casarin, M.; Lanza, A.; Nestola, F.; Pandolfo, L.; Pettinari, C.; Scatena, R. Reaction of Copper(II) Chloroacetate with Pyrazole. Synthesis of a One-Dimensional Coordination Polymer and Unexpected Dehydrochlorination Reaction. *Cryst. Growth Des.* **2015**, *15*, 5910−5918.
(36) Rivera-Carrillo, M.; Chakraborty, I.; Raptis, R. G. Systematic Synthesis of a Metal Organic Framework Based on Triangular Cu3(μ3-OH) Secondary Building Units: From a 0-D Complex to a 1-D Chain and a 3-D Lattice. *Cryst. Growth Des.* **2010**, *10*, 2606−2612.
(37) Di Nicola, C.; Garau, F.; Gazzano, M.; Guedes da Silva, M. F. C.; Lanza, A.; Monari, M.; Nestola, F.; Pandolfo, L.; Pettinari, C.; Pombeiro, A. J. L. New Coordination Polymers and Porous Supramolecular Metal Organic Network Based on the Trinuclear Triangular Secondary Building Unit [Cu3(μ3-OH)(μ-pz)3]2+ and 4,4′-Bypiridine. 1°. *Cryst. Growth Des.* **2012**, *12*, 2890−2901.
(38) Pandolfo, L. *Advances in Organometallic Chemistry and Catalysis. The Silver/Gold International Conference on Organometallic Chemistry Celebratory Book*; Pombeiro, A. J. L., Ed.; Wiley. 2014' *part 4*, pp 407−419.

https://doi.org/10.1021/acs.cgd.1c00861
Cryst. Growth Des. 2022, 22, 1032−1044

(39) Di Nicola, C.; Garau, F.; Gazzano, M.; Lanza, A.; Monari, M.; Nestola, F.; Pandolfo, L.; Pettinari, C. Interaction of the Trinuclear Triangular Secondary Building Unit [Cu3(μ3-OH)(μ-pz)3]2+ with 4,4′-Bipyridine. Structural Characterizations of New Coordination Polymers and Hexanuclear CuII Clusters. 2°. *Cryst. Growth Des.* **2015**, *15*, 1259−1272.
(40) Condello, F.; Garau, F.; Lanza, A.; Monari, M.; Nestola, F.; Pandolfo, L.; Pettinari, C. Synthesis and Structural Characterizations of New Coordination Polymers Generated by the Interaction Between the Trinuclear Triangular SBU [Cu3(μ3-OH)(μ-pz)3]2+ and 4,4′-Bipyridine. 3°. *Cryst. Growth Des.* **2015**, *15*, 4854−4862.
(41) Shi, K.; Mathivathanan, L.; Drozd, V. A.; Raptis, R. G. Three Topological Isomers of 1D- and 2D-Coordination Polymers Consisting of Tricopper Pyrazolate SBUs and 4,4′-Trimethylenedipyridine Linkers: Effect of Pressure on the Structure. *Cryst. Growth Des.* **2019**, *19*, 381−390.
(42) Di Nicola, C.; Forlin, E.; Garau, F.; Lanza, A.; Natile, M. M.; Nestola, F.; Pandolfo, L.; Pettinari, C. Coordination polymers based on trinuclear and mononuclear copper-pyrazolate building moieties connected by fumarate or 2-methylfumarate ions. *J. Organomet. Chem.* **2012**, *714*, 74−80.
(43) Zhang, H.; Lu, Y.; Zhang, Z.; Wang, E. A three-dimensional metal−organic framework based on hexanuclear copper units with unsaturated CuII centers. *Inorg. Chem. Commun.* **2012**, *17*, 9−12.
(44) Di Nicola, C.; Forlin, E.; Garau, F.; Gazzano, M.; Lanza, A.; Monari, M.; Nestola, F.; Pandolfo, L.; Pettinari, C.; Zorzi, A.; Zorzi, F. Coordination Polymers Based on the Trinuclear Triangular Secondary Building Unit [Cu3(μ3-OH)(μ-pz)3]2+ (pz = pyrazolate) and Succinate Anion. *Cryst. Growth Des.* **2013**, *13*, 126−135.
(45) Bala, S.; Bhattacharya, S.; Goswami, A.; Adhikary, A.; Konar, S.; Mondal, R. Designing Functional Metal−Organic Frameworks by Imparting a Hexanuclear Copper-Based Secondary Building Unit Specific Properties: Structural Correlation With Magnetic and Photocatalytic Activity. *Cryst. Growth Des.* **2014**, *14*, 6391−6398.
(46) Zhang, T.; Lu, Y.; Zhang, Z.; Lan, Q.; Liu, D.; Wang, E. Single-crystal to single-crystal transformation from a hydrophilic−hydrophobic metal−organic framework to a layered coordination polymer. *Inorg. Chim. Acta* **2014**, *411*, 128−133.
(47) Zhao, N.; Yang, L.; Pan, Q.; Han, J.; Li, X.; Liu, M.; Wang, Y.; Wang, X.; Pan, Q.; Zhu, G. Step-by-Step Assembly of Metal−Organic Frameworks from Trinuclear Cu3 Clusters. *Inorg. Chem.* **2019**, *58*, 199−203.
(48) Boudalis, A. K.; Rogez, G.; Heinrich, B.; Raptis, R. G.; Turek, P. Towards ionic liquids with tailored magnetic properties: bmim+ salts of ferro- and antiferromagnetic CuII3 triangles. *Dalton Trans.* **2017**, *46*, 12263−12273.
(49) Mathivathanan, L.; Boudalis, A. K.; Turek, P.; Pissas, M.; Sanakis, Y.; Raptis, R. G. Interactions between H-bonded [CuII3(μ3-OH)] triangles; a combined magnetic susceptibility and EPR study. *Phys. Chem. Chem. Phys.* **2018**, *20*, 17234−17244.
(50) Akhtar, S.; Bala, S.; De, A.; Das, K. S.; Adhikary, A.; Jyotsna, S.; Poddar, P.; Mondal, R. Designing Multifunctional MOFs Using the Inorganic Motif [Cu3(μ3-OH)(μ-Pyz)] as an SBU and Their Properties. *Cryst. Growth Des.* **2019**, *19*, 992−1004.
(51) Zheng, L.; Yang, R.; Zhou, A.; Hu, S. A New 2-D Organometallic Framework Constructed with Delocalizing π Electronic Trinuclear Units. *J. Clust. Sci.* **2019**, *30*, 507−512.
(52) *CRC Handbook of Chemistry and Physics*, 84th ed.; 2003−2004.
(53) Koizumi, H.; Osaki, K.; Watanabé, T. Crystal Structure of Cupric Benzoate Trihydrate Cu(C6H5COO)23H2O. *J. Phys. Soc. Jpn.* **1963**, *18*, 117−124.
(54) Macrae, C. F.; Edgington, P. R.; McCabe, P.; Pidcock, E.; Shields, G. P.; Taylor, R.; Towler, M.; van de Streek, J. Mercury: visualization and analysis of crystal structures. *J. Appl. Crystallogr.* **2006**, *39*, 453−457.
(55) Macrae, C. F.; Bruno, I. J.; Chisholm, J. A.; Edgington, P. R.; McCabe, P.; Pidcock, E.; Rodriguez-Monge, L.; Taylor, R.; van de Streek, J.; Wood, P. A. Mercury CSD 2.0 - new features for the visualization and investigation of crystal structures. *J. Appl. Crystallogr.* **2008**, *41*, 466−470.
(56) Deacon, G. B.; Phillips, R. J. Relationships between the carbon-oxygen stretching frequencies of carboxylato complexes and the type of carboxylate coordination. *Coord. Chem. Rev.* **1980**, *33*, 227−250.
(57) Svorec, J.; Polakovicová, P.; Moncol, J.; Kuchtanin, V.; Breza, M.; Soralova, S.; Padelková, Z.; Mrozinski, J.; Lis, T.; Seglá, P. Structural, magnetic and quantum-chemical study of dinuclear copper(II) thiophenecarboxylate and furancarboxylate complexes. *Polyhedron* **2014**, *81*, 216−226.
(58) Casarin, M.; Cingolani, A.; Di Nicola, C.; Falcomer, D.; Monari, M.; Pandolfo, L.; Pettinari, C. The Different Supramolecular Arrangements of the Triangular [Cu3(μ3-OH)(μ-pz)3]2+ (pz = Pyrazolate) Secondary Building Units. Synthesis of a Coordination Polymer with Permanent Hexagonal Channels. *Cryst. Growth Des.* **2007**, *7*, 676−685.
(59) Di Nicola, C.; Garau, F.; Gazzano, M.; Monari, M.; Pandolfo, L.; Pettinari, C.; Pettinari, R. Reactions of a Coordination Polymer Based on the Triangular Cluster [Cu3(μ3-OH)(μ-pz)3]2+ with Strong Acids. Crystal Structure and Supramolecular Assemblies of New Mono-, Tri-, and Hexanuclear Complexes and Coordination Polymers. *Cryst. Growth Des.* **2010**, *10*, 3120−3131.
(60) Angaridis, P. A.; Baran, P.; Boča, R.; Cervantes-Lee, F.; Haase, W.; Mezei, G.; Raptis, R. G.; Werner, R. Synthesis and Structural Characterization of Trinuclear CuII−Pyrazolato Complexes Containing μ3-OH, μ3-O, and μ3-Cl Ligands. Magnetic Susceptibility Study of [PPN]2[(μ3-O)Cu3(μ-pz)3Cl3]. *Inorg. Chem.* **2002**, *41*, 2219−2228.
(61) Boča, R.; Dlháň, L.; Mezei, G.; Ortiz-Pérez, T.; Raptis, R. G.; Telser, J. Triangular, Ferromagnetically-Coupled CuII3−Pyrazolato Complexes as Possible Models of Particulate Methane Monooxygenase (pMMO). *Inorg. Chem.* **2003**, *42*, 5801−5803.
(62) Yang, L.; Powell, D. R.; Houser, R. P. Structural variation in copper(i) complexes with pyridylmethylamide ligands: structural analysis with a new four-coordinate geometry index, τ4. *Dalton Trans.* **2007**, 955−964.
(63) Addison, A. W.; Rao, N. T.; Reedijk, J.; van Rijn, J.; Verschoor, G. C. Synthesis, structure, and spectroscopic properties of copper(II) compounds containing nitrogen−sulphur donor ligands; the crystal and molecular structure of aqua[1,7-bis(N-methylbenzimidazol-2′-yl)-2,6-dithiaheptane]copper(II) perchlorate. *J. Chem. Soc., Dalton Trans.* **1984**, 1349−1356.
(64) Okuniewski, A.; Rosiak, D.; Chojnacki, J.; Becker, B. Coordination polymers and molecular structures among complexes of mercury(II) halides with selected 1-benzoylthioureas. *Polyhedron* **2015**, *90*, 47−57.
(65) Steiner, T. The Hydrogen Bond in the Solid State. *Angew. Chem., Int. Ed.* **2002**, *41*, 48−76.
(66) Ozarowski, A.; Calzado, C. J.; Sharma, R. P.; Kumar, S.; Jezierska, J.; Angeli, C.; Spizzo, F.; Ferretti, V. Metal−Metal Interactions in Trinuclear Copper(II) Complexes [Cu3(RCOO)4(H2TEA)2] and Binuclear [Cu2(RCOO)2(H2TEA)2]. Syntheses and Combined Structural, Magnetic, High-Field Electron Paramagnetic Resonance, and Theoretical Studies. *Inorg. Chem.* **2015**, *54*, 11916−11934.
(67) Ray, M. S.; Bhattacharya, R.; Chaudhuri, S.; Righi, L.; Bocelli, G.; Mukhopadhyay, G.; Ghosh, A. Synthesis, characterisation and X-ray crystal structure of copper(II) complexes with unsymmetrical tetradentate Schiff base ligands: first evidence of Cu(II) catalysed rearrangement of unsymmetrical to symmetrical complex. *Polyhedron* **2003**, *22*, 617−624.
(68) Yang, Y.; Mims, C. A.; Disselkamp, R. S.; Kwak, J.-H.; Peden, C. H. F.; Campbell, C. T. (Non)formation of Methanol by Direct Hydrogenation of Formate on Copper Catalysts. *J. Phys. Chem. C* **2010**, *114*, 17205−17211.
(69) Jenniefer, S. J.; Muthiah, P. T. Synthesis, characterization and X-ray structural studies of four copper (II) complexes containing dinuclear paddle wheel structures. *Chem. Centr. J.* **2013**, *7*, 35.

https://doi.org/10.1021/acs.cgd.1c00861
Cryst. Growth Des. 2022, 22, 1032−1044

(70) Del Sesto, R. E.; Arif, A. M.; Miller, J. S. Copper(II) Benzoate Nitroxide Dimers and Chains: Structure and Magnetic Studies. *Inorg. Chem.* **2000**, *39*, 4894−4902.
(71) Bhowmik, P.; Chattopadhyay, S.; Ghosh, A. Synthesis and structure of mono-, di- and tri-nuclear copper(II) benzoate complexes with a tridentate N2O donor Schiff base ligand. *Inorg. Chim. Acta* **2013**, *396*, 66−71.
(72) http://rcsr.anu.edu.au/nets/pts.
(73) Ledezma-Gairaud, M.; Pineda, L. W. Bis(μ2-benzoato-κ2O,O′)bis(benzoato-κO)bis(ethanol-κO)bis(μ3-hydroxido)hexakis-(μ-pyrazolato-κ2N,N′)hexacopper(II) ethanol disolvate. *IUCrData* **2019**, *4*, x191190.

https://doi.org/10.1021/acs.cgd.1c00861
Cryst. Growth Des. 2022, 22, 1032−1044